

## Unraveling the mechanism of multicopper oxidases : from ensemble to single molecule

Gupta, A.

#### Citation

Gupta, A. (2014, April 29). *Unraveling the mechanism of multicopper oxidases : from ensemble to single molecule*. Retrieved from https://hdl.handle.net/1887/25397

Version: Not Applicable (or Unknown)

License: Leiden University Non-exclusive license

Downloaded from: <a href="https://hdl.handle.net/1887/25397">https://hdl.handle.net/1887/25397</a>

**Note:** To cite this publication please use the final published version (if applicable).

#### Cover Page



### Universiteit Leiden



The handle <a href="http://hdl.handle.net/1887/25397">http://hdl.handle.net/1887/25397</a> holds various files of this Leiden University dissertation

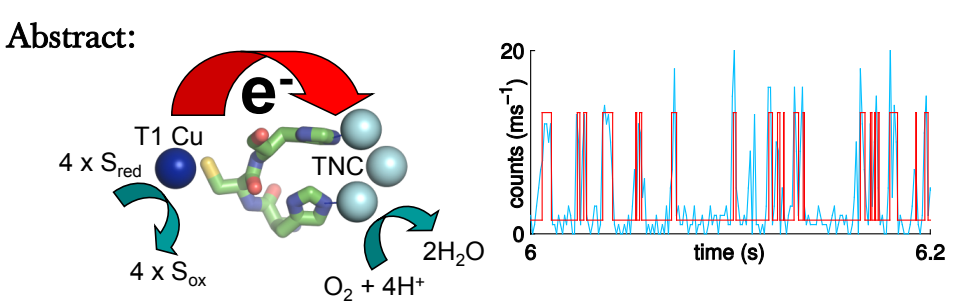
Author: Gupta, Ankur

Title: Unraveling the mechanism of multicopper oxidases: from ensemble to single

molecule

**Issue Date:** 2014-04-29

# One at a Time: Intramolecular Electron-Transfer Kinetics in Small Laccase observed during turnover\*



Single-molecule enzymology provides an unprecedented level of detail about enzyme mechanisms, which have been very difficult to probe in bulk. One such aspect is intramolecular electron transfer (ET) which is a recurring theme in the research on oxidoreductases containing multiple redox-active sites. We measure the intramolecular ET rates between the copper centers of the small laccase (SLAC) from *Streptomyces coelicolor* at room temperature and pH 7.4, one molecule at a time, during turnover. The forward and backward rates across many molecules follow a log-normal distribution with means of 460 s<sup>-1</sup> and 85 s<sup>-1</sup>, respectively, corresponding to activation energies of 347 and 390 meV for the forward and backward rates. The driving force and the reorganization energy amount to 0.043 eV and 1.5 eV, respectively. The spread in rates corresponds to a spread of ~30 meV in the activation energy. The second-order rate constant for reduction of the T1 site amounts to 2.9x10<sup>4</sup> M<sup>-1</sup>s<sup>-1</sup>. The mean of the distribution of forward ET rates is higher than the turnover rate from ensemble steady-state measurements and, thus, is not rate limiting.

\*Adapted from: Gupta, A.; Aartsma, T.J.; Canters, G.W. J. Am. Chem. Soc. **2014**, *136*, 2707.

#### 4.1 Introduction

Efficient and controlled electron transfer (ET) is essential for the proper course of metabolic processes like energy conversion and storage. Traditionally, ET rates in proteins are measured under single-turnover conditions using techniques like pulse radiolysis or flash photolysis, and the results are sometimes not in agreement with the results of steady-state kinetics measurements. Study of enzyme kinetics at the single-molecule (SM) level allows direct access to real-time events under steady-state conditions. SM techniques and the underlying theoretical framework have evolved rapidly and greatly advanced our knowledge of enzyme mechanisms over the past decade. The redox kinetics of flavin-containing cholesterol oxidase and pentaerythritol tetranitrate reductase, Cu-containing nitrite reductases, and the conformational dynamics of dihydrofolate reductase, for instance, have been studied profitably by SM techniques. In this chapter, we report the first SM measurements of the ET rate between the copper centers of a multicopper oxidase (MCO), *i.e.*, small laccase (SLAC) from *Streptomyces coelicolor*.

MCOs catalyze the four-electron reduction of O2 to H2O concomitant with oxidation of substrate molecules. Laccases belong to the family of MCOs which have been commercialized by industry owing to their ability to oxidize a wide variety of substrates. Their enzymatic machinery consists of a type 1 (T1) Cu which accepts reducing equivalents from substrate molecules and transfers them across ~13 Å via a conserved HisCysHis motif to the trinuclear Cu cluster (TNC), where O<sub>2</sub> is converted to H<sub>2</sub>O. <sup>14,15</sup> The TNC is traditionally considered to be composed of a binuclear type 3 (T3) Cu pair and a normal type 2 (T2) Cu. A crucial step in the catalytic process is the transfer of an electron from the T1 Cu to the TNC, one at a time, four times to complete a turnover. Several reports exist in the literature focusing on measuring the ET rates anaerobically using pulse radiolysis and flash photolysis under single-turnover conditions. <sup>2,3,16-18</sup> The pioneering studies of Farver, Pecht and coworkers, for instance, greatly advanced our understanding of how the electrons move and equilibrate between different redox centers and the consequences of these dynamics on the enzyme mechanism. However, close evaluation of these studies reveals that the measured ET rates are sometimes an order of magnitude or more lower than the turnover rates. <sup>2,16</sup> Although measurements under single-turnover conditions can provide valuable information about the enzyme mechanism, the observed intermediates are not necessarily similar to the intermediates occurring during steady-state turnover. Thus, there is a continuous demand for new methods to measure the ET rates during turnover.

Recently, a new principle was introduced: fluorescence-based detection of protein redox state(s) (FluRedox),<sup>19</sup> which allows monitoring the redox state changes of oxido-reductases during turnover at a high temporal resolution and at the SM level.<sup>10-12</sup> Not only does this method allow the study of hidden aspects of enzyme kinetics/dynamics (which are often masked by the rate-determining step in a bulk measurement), it also allows the study of the heterogeneity in a population of molecules. We make use of this principle to study the ET in SLAC.

SLAC is a homotrimer in which each monomer consists of two cupredoxin domains (Figure 1a) unlike the more common MCOs, which are three- or six-domain monomeric proteins. However, it has a similar active-site morphology consisting of T1 and TNC sites and catalyzes the same reaction as other MCOs. It has been proposed that such trimeric proteins are evolutionary precursors to ascorbate oxidase, the 3-domain laccases and the 6-domain ceruloplasmin. Recently, it was shown that SLAC may also differ from the common laccases in its mechanism of O<sub>2</sub> reduction, wherein a redox-active tyrosine residue (Y108) may have a participatory role. ALAC has been structurally characterized have a participatory role. SLAC has been system, provides excellent opportunities to study the ET in this enzyme in great detail.

#### 4.2 Results and Discussion

To selectively label SLAC, K204C and R203C variants were prepared which contain a surface–exposed cysteine available for conjugation with thiol–reactive dyes and linkers.<sup>26</sup> When oxidized, the enzyme exhibits absorption bands at 330 and 590 nm, the latter characteristic of the T1 Cu site. The 590 nm absorption

overlaps with the emission of the Atto647N dye; thus, when using SLAC labeled with this dye, the fluorescence of the dye is quenched by means of Förster resonance energy transfer (FRET) from the fluorophore to the T1 Cu chromophore. The 590 nm absorption band is absent when the enzyme is reduced in which case the fluorescence is recovered. Thus, the emission from the enzyme–dye conjugate can serve as a highly sensitive probe of the redox state of the T1 Cu. Such fluorescence switching of the labeled variants was verified in bulk when the enzyme was cycled between oxidized and reduced states (Figure S3). Both the R203C and K204C variants showed similar fluorescence switching but further experiments focused on the K204C variant. The enzyme was conjugated with thiol–reactive biotin–PEG linkers to make it suitable for surface immobilization. A cartoon depicting the labeling strategy is shown in Figure 1a.

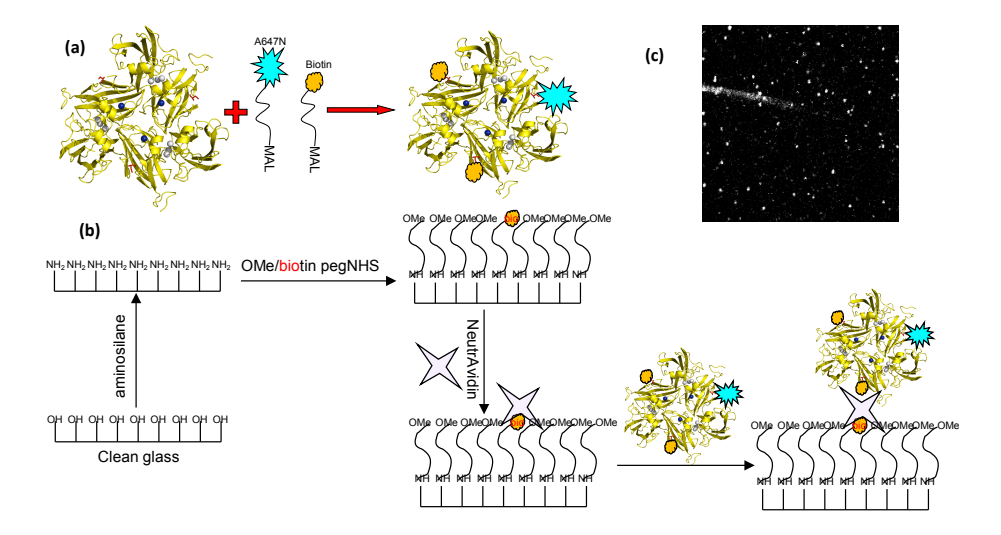


**Figure 1:** (a) K204C variant of SLAC conjugated with Atto647N–maleimide and biotin–PEG–maleimide. The conditions are chosen so that the dye–to–protein labeling ratio does not exceed 5 % to ensure most enzyme molecules carry only one or no fluorescence label. T1 Cu is depicted in blue, TNC in grey and Cys204 in red. (b) Functionalization of glass coverslips with aminosilane and PEG linkers and immobilization of SLAC conjugates using the NeutrAvidin–biotin interaction. (c) A 40x40 μm² image taken under a confocal fluorescence microscope of the sample prepared in (b). The bright spots are individual SLAC molecules. For details about conjugation, immobilization, and confocal setup, see Supplementary Information.

SLAC molecules must be immobilized on a transparent solid support before any measurements can be made on a confocal microscope. A number of methods are described in the literature for immobilization of proteins on a surface. 27-29 It was an additional interest for us to immobilize SLAC in a site-specific manner. To achieve this, the glass coverslips were functionalized as shown in Figure 1b.<sup>26</sup> first functionalized with Briefly, clean coverslips were 3 - (2 aminoethyl)aminopropyl trimethoxysilane to create an amine-terminated hydrophilic surface. This functionalized surface was further treated with polyethylene glycol (PEG) linkers containing an amine-reactive end (NHS ester) and a biotin or methoxy group at the other terminus. It was demonstrated previously that the PEG linkers minimize non-specific adsorption of the protein on the surface.<sup>30,32</sup> The ratio of biotin-terminated PEG to methoxy-terminated PEG on the surface was kept below 0.1%. The SLAC conjugates prepared earlier were then tethered to the surface via biotin–NeutrAvidin interactions (Figure 1b). This labeling and immobilization strategy helps ensure that the label/linkers attach to the protein at a specific site and minimize any heterogeneity in the sample preparation. A typical confocal image of immobilized SLAC molecules on a coverslip prepared by the above method is shown in Figure 1c.

When the laser is focused on one of the molecules, the variation in fluorescence count rate with time can be observed. In the absence of substrate, the fluorescence intensity is low and, apart from statistical noise, no fluorescence fluctuations are observed, indicating that the enzyme is in a stable oxidized state (Figure S4). In the presence of excess reductant under aerobic conditions and with the TNC selectively inhibited by incubation with cyanide, a high fluorescence intensity is observed and no fluctuations are observed, either (Figure S4), indicating that the T1 site is in a stably reduced state. The two experiments demonstrate that ET between the excited label and the T1 Cu in either the reduced or the oxidized form does not occur at a measurable rate. However, aerobic conditions and in the presence of N,N-dimethyl-punder phenylenediamine (DMPD) as a mediator and ascorbate as a substrate, the enzyme starts to turn over, and discrete fluctuations in the emission count rates are observed.<sup>26</sup> A typical measurement is shown in Figures 2a,b. We ascribe these fluctuations to ET from the T1 Cu to the TNC (high to low fluorescence)

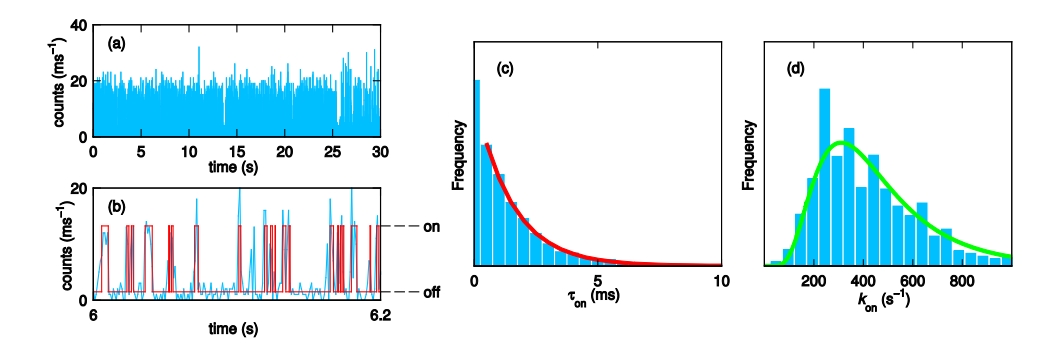


**Figure 2:** (a) Typical binned time trace (1 ms bin time) of a turning over single SLAC molecule. The molecule shows fluctuations between the high and low emission rates as the redox state of T1 Cu changes, which can be seen from a small portion of the trace as shown in (b). The red trace in (b) is bin-free and was obtained from the changepoint analysis. (c) The dwell time  $(\tau_{on})$  distribution of the molecule in the on-state from the trace shown in (a). The number of "on" intervals present in this trace amounted to 2767. The red line is the monoexponential fit to the normalized data with a decay constant  $k_{on} = 660 \text{ s}^{-1}$ . (d) Distribution of  $k_{on}$  obtained from ~720 molecules of SLAC. The green line is the fit corresponding to a log-normal distribution with a mean value of 450 s<sup>-1</sup>. The measurements reported in panels (a)–(c) were made in 20 mM MOPS buffer (pH 7.4) and at 20 °C with DMPD and ascorbate concentrations of 5 and 10 mM, respectively. The data reported in panel (d) represent measurements that were performed at concentrations of DMPD varying from 0.02 to 5 mM.

and from the substrate or the TNC to the T1 Cu (low to high fluorescence).

Data were collected in a photon-by-photon manner. Since only the arrival times are recorded, it is common to bin the data to visualize the count rate fluctuations. Such binning generally limits the time resolution of the experimental analysis. Thus, we made use of a bin-free method, a so-called changepoint analysis, which utilizes Bayesian statistics to analyze the raw data and to determine the time points when the molecule switches from one state to another.<sup>33</sup> It is evident from Figure 2b that the red trace obtained by such an analysis overlaps well with the binned trace. Thereafter, the dwell times in the on-state were binned, and a histogram of these dwell times was obtained (Figure 2c).<sup>26</sup> As can be seen from the fit in Figure 2c, the distribution of dwell times in the on-state follows a single-exponential decay and directly provides a rate constant (~660 s<sup>-1</sup> in this

example) which we equate to the rate of ET from T1 to TNC, denoted by  $k_{\text{T1}\rightarrow\text{TNC}} \equiv k_{\text{on}}$ . We measured time trajectories of ~720 molecules where the DMPD concentration was varied between 0.02 and 5 mM and obtained ET rate constants in the manner discussed above. It appears that the logarithm of the rate constants can be well fitted by a Gaussian distribution (Figure S7). Thus, the rate constants follow a log-normal distribution with an arithmetic mean of  $k_{\text{T1}\rightarrow\text{TNC}} = 460 \text{ s}^{-1}$ , corresponding to a normal distribution of activation energies.<sup>34</sup> The distribution of ET rates appears quite broad and demonstrates the heterogeneity that exists from one molecule to another (*vide infra*). While in bulk experiments the catalytic reaction rate depends on substrate concentration, it is gratifying to note that the  $k_{\text{on}}$  distributions are concentration independent (Figure S8a,b), which confirms that we are dealing with an intramolecular process.

In a similar way, the off-times were analyzed. Since they appear dependent on the DMPD concentration, they could not be combined into a single data set for analysis as had been done for the on-time analysis (see above). The data sets obtained at 50  $\mu$ M and 5 mM DMPD were large enough to allow a preliminary analysis, which resulted in  $k_{\text{TNC}\to\text{T1}} = 85 \text{ s}^{-1}$  and a second order rate constant  $k_{\text{s}} = 2.9 \times 10^4 \text{ M}^{-1} \text{s}^{-1}$ . From the ratio of the two internal ET rate constants and associated variances, a driving force of 43 meV can be derived. The bimolecular rate constant is smaller than the rate constant measured in the bulk  $(1.3 \times 10^5 \text{ M}^{-1} \text{ s}^{-1})$ ; Figure S2). We ascribe the difference to how the enzyme is present: free in solution vs. labeled and immobilized on a solid support.

A number of features are worth pointing out. First, the waiting time distributions can be fit by monoexponential decays (see Figure 2c, for example). Apparently, on the time scale of the experiment (0.5–120 s) the distribution of ET rates (Figure 2d) is static. Second, since four ET steps are needed to complete the enzyme cycle, the differences between the *k*'s for the different steps must be small (<20% of the mean). This is in line with relatively small changes in driving force for the T1–TNC ET step as the TNC fills up with electrons.<sup>35</sup> Third, the internal ET rate is larger than the turnover rate measured under substrate saturating conditions in the bulk (Figure S2). This means that the frequent transitions between on– and off–states that we observe are due, in large measure, to jumps

of electrons back and forth between the TNC and the T1 site. Moreover, since no long on–times (of the duration of the enzyme turnover time) were observed, a long–lived four–electron–reduced state is not part, apparently, of the enzyme cycle. It is conceivable that, after loading the TNC with two or three electrons, charge compensation is necessary through the uptake of protons and/or through dehydroxylation involving a rearrangement of the water and H–bonding network around the TNC before any further electrons can enter the T1 site. Another possibility is that a reversible conformational change temporarily switches off the T1 site, as suggested for the homologous Cu–containing nitrite reductase.<sup>36</sup> A more extensive exploration of this finding must await further experiments.

The distribution in rates may be connected with intrinsic and extrinsic causes. Enzyme immobilization on solid surfaces may lead to (partial) loss of activity. In the present study, we investigate only enzyme molecules that were still active after immobilization. The distribution of forward ET rates in Figure 2d is ascribed, thus, to intrinsic causes and is related to the thermodynamics of the catalytic process. In view of the average distance between the T1 Cu and the TNC (~13 Å) and the distance dependence of the electronic coupling  $(H_{DA})$ between the donor (T1 Cu) and the acceptor (TNC) ( $H_{DA} = k_0 \exp{-\beta (r - r_0)}$ ) we can calculate (with  $\beta = 1 \text{ Å}^{-1}$ ) an activationless ( $\Delta G^0 = -\lambda$ ) ET rate constant  $k^0 = 3.7 \times 10^8 \text{ s}^{-1.26}$  Using semiclassical Marcus theory and mean and variance of the  $k_{\rm on}$  distribution obtained from Figure 2d, an estimate of 0.347 eV for the activation energy  $(\Delta G^{\ddagger})$  can be calculated. Using a value of 43 meV for the driving force a value for the reorganization energy  $\lambda = 1.5$  eV is obtained which is in line with the reorganization energy of other metalloenzymes including laccases.  $^{26,1,37\cdot39}$  The spread in the activation energy, corresponding to the  $k_{\rm on}$ distribution, amounts to  $\pm$  28 meV, which would be equivalent to a spread in the driving force of  $\pm$  56 meV or a spread in  $\lambda$  of  $\pm$  110 meV.

A similar analysis can be performed for the back ET rates. The rates obtained at  $[DMPD] = 50 \, \mu M$  can be used for this purpose since the contribution of the bimolecular reaction to the observed rates is negligibly small in this case. We find an activation energy of 390 meV with a spread of  $\pm$  25 meV, which leads to

a value for the reorganization energy of  $\lambda = 1.5$  eV. As expected, the spread in activation energies for the forward and backward ET is the same within the experimental uncertainty.

Gray and Winkler argued that, with the available experimental and theoretical methods, it is difficult to obtain values of  $\lambda$  to a precision that is better than  $\pm$  100 meV.<sup>37</sup> It is surprising to realize that such a small uncertainty is compatible with the distribution in ET rates that is observed in the present SM measurements. Thus, the distribution that initially appears quite broad relates to a rather narrow distribution of  $\Delta G^{\ddagger}$  ( $\pm$  28 meV). A similar observation was reported earlier for copper proteins.<sup>40,41</sup>

In pulse radiolysis experiments on SLAC under anaerobic conditions, it was reported that the ET rate increases as the TNC acquires electrons, one at a time. 17 Moreover, the smallest and the largest ET rates that could be measured in those experiments amounted to ~ 15 and 186 s<sup>-1</sup>, respectively. However, within the time resolution of the current measurements under turnover or aerobic conditions, we do not observe such a variation of ET rates, as the dwell time distribution fits to a single exponential (vide supra). Moreover, in the ensemble steady-state measurements at pH 6, enzymatic rates in excess of 300 s<sup>-1</sup> were measured, which is faster than the ET rate that could be obtained from the pulse radiolysis experiments.<sup>25</sup> It has been shown for ascorbate oxidase that the presence of oxygen enhances the ET rate by structural perturbation of the TNC. <sup>2,3</sup> Very recently, it was demonstrated with stopped-flow measurements on Rhus vernicifera laccase that the so-called native intermediate (or freshly cycled enzyme) is capable of transferring electrons (from T1 Cu to TNC) at a much higher rate than the resting enzyme.<sup>39</sup> Although the "cycled" form of SLAC was used in the pulse radiolysis experiments, the experimental setup may not allow the experiment to proceed quickly enough so as to prevent the (partial) decay of the native intermediate to the resting form of SLAC. This might explain the difference between the pulse radiolysis and the current experiments. Nevertheless, the above points clearly emphasize the fact that a more reliable way to measure such a rate would be to do it during the enzyme turnover.

We are in the process of performing more experiments to analyze the correlation with the bulk measurements. The method reported here may be applicable to study ET in virtually any redox enzyme with a suitable fluorophore, provided that the enzyme exhibits distinctly different absorption spectra in the reduced and oxidized states.

#### 4.3 Supplementary Information

Site-directed mutagenesis: In order to be able to attach a label or a linker to the protein surface a cysteine was introduced into the sequence of the protein. Notice that the native enzyme does not contain any cysteines except for Cys288 which is one of the ligands of the type 1 Cu and which is not accessible for external reactive groups. Site-directed mutagenesis was carried out using the Quick Change site-directed mutagenesis kit (Stratagene). The primers used for respective mutations are given below where mutations are in bold and underlined.

#### R203C

Forward primer: 5'— G ACC ATC AAC AAC TGC AAG CCG CAC

ACC G -3'

Reverse primer: 5'— C GGT GTG CGG CTT GCA GTT GAT

GGT C -3'

#### K204C

Forward primer: 5'— G ACC ATC AAC AAC CGC <u>TGT</u> CCG CAC ACC GGC CCC GAC -3'

Reverse primer: 5'— GTC GGG GCC GGT GTG CGG ACA GCG GTT GTT GAT GGT C —3'

Desired mutations were confirmed by DNA sequencing (BaseClear). The position/distance of the residue for mutation was chosen so that the fluorophore can be expected not to undergo any redox chemistry or photoinduced electron transfer with the T1 Cu but at the same time is within the Förster radius to enable highly selective sensing of the desired T1 Cu.

The purification of the mutants was carried out as reported previously.<sup>20</sup> The proteins were aliquoted and stored at -80 °C till further use. The absorption spectra of the *wt*-SLAC, K204C and R203C variants are shown in Figure S1.

**Steady-state kinetics:** Bulk steady state kinetics measurements were performed as reported earlier with a slight modification.<sup>25</sup> Instead of TMPD (*N,N,N',N'* 

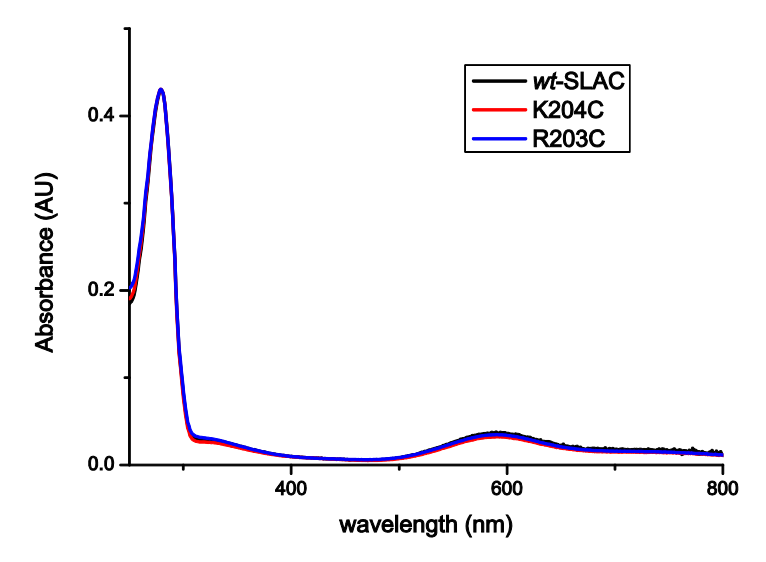


**Figure S1:** Absorption spectra of the oxidized *wt*–SLAC overlaid with those of K204C and R203C in 20mM sodium phosphate buffer (pH 7.4) at ambient temperature. The spectra have been normalized at the 280nm absorption.

tetramethyl-p-phenylenediamine), DMPD (N,N dimethyl-p-phenylenediamine) was used as substrate in the presence of 10mM ascorbate. Variations in the concentration of ascorbate had no effect on enzyme activity as the reaction with ascorbate is too slow to reduce T1 Cu directly. The presence of ascorbate had an unintended advantage in that it kept the solution colorless which aided in establishing the fluorescence assays. Typical plots of the catalytic rates vs substrate concentration are shown in Figure S2.

Labeling SLAC mutants: The engineered thiols were activated by incubating the enzyme with 5–10 equivalents of TCEP (*tris*(2–carboxyethyl)phosphine) or DTT (dithiothreitol). The following steps were performed as quickly as possible as the thiols have a tendency to get oxidized in the presence of air. Excess reductant was removed by gel filtration (HiTrap Desalting column, GE). At the same time the buffer was exchanged to 20mM Sodium phosphate (pH 7.4) if the sample was not already in this buffer. About 0.25 equivalents of Atto647N–maleimide were added to the protein solution and the reaction was allowed to proceed on ice for 1–2 minutes. Immediately afterwards, a large excess of biotin–PEG–maleimide (MW 3400, LaysanBio) linker was added to quench the excess

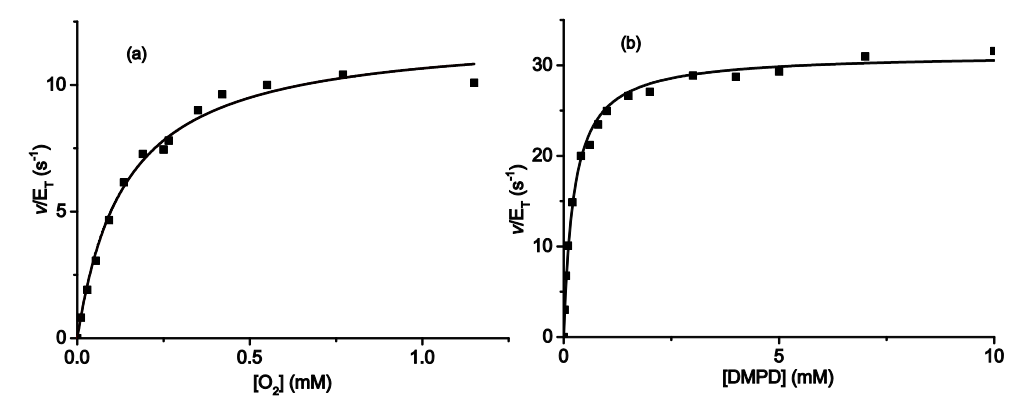
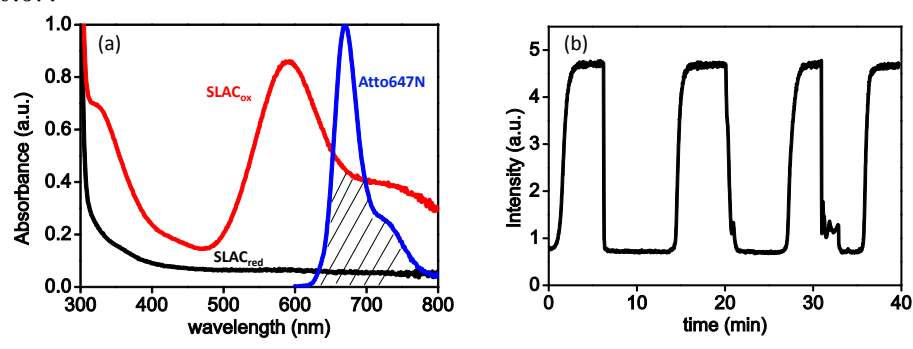


Figure S2: (a) Plot of  $O_2$  consumption rates plotted against the respective  $O_2$  concentration while keeping the initial DMPD and ascorbate concentrations fixed at 5 mM and 10mM, respectively, for each measurement. The solid line is a fit of the data to the Michaelis-Menten equation which yields  $v_{\rm max}=12~{\rm s}^{-1}$  and  $K_{\rm M}$  ( $O_2$ ) = 130  $\mu$ M. (b) Plot of DMPD oxidation rate plotted against the respective DMPD concentration at air saturation (i.e. around 260  $\mu$ M  $O_2$ ). No ascorbate was used in this measurement. The solid line is a fit of the data to the Michaelis-Menten equation which yields  $v_{\rm max}=31~{\rm s}^{-1}$ ,  $K_{\rm M}$  (DMPD) = 235  $\mu$ M and  $k_{\rm S}=1.3~{\rm x}~10^5~{\rm M}^{-1}{\rm s}^{-1}$ . The measurements were made in 200mM sodium phosphate (pH 7.4) at 22  $^{0}$ C.

of thiols on the protein. This serves a dual purpose: the protein may not dimerize or aggregate by forming inter-protein disulfide bonds and a biotin group is present at the end of the linker, which can be used in combination with Avidin to immobilize the protein on the surface. The reaction was further allowed to proceed in the dark on ice for 30 minutes. The excess of dye and linkers was removed by gel filtration and the degree of labeling was estimated from the absorption spectrum of the protein. It was necessary to ensure that the degree of labeling with the fluorophore be kept very low (in our case we kept it at less than 5%) so that most molecules will carry only one fluorophore or no fluorophore at all. The protein conjugates were not purified further to separate labeled from unlabeled protein as the unlabeled protein would not be visible in the fluorescence microscope anyway and would not affect our results. Since an excess of biotin-PEG linker was used, the majority of the proteins will carry two or three linkers. Again, no attempts were made to separate the various species. The samples were aliquoted and stored at -80 °C till further use.

Fluorescence switching in bulk: To establish that the fluorescence of the dye-conjugated protein is sensitive to the redox state of the protein, steady-state fluorescence measurements were made in bulk. Upon excitation with 645 nm light, the fluorescence intensity was found to switch between high and low states when the enzyme was reduced and oxidized successively. An example of this switching is shown in Figure S3. We checked that the fluorophore itself or the unconjugated fluorophore in the presence of protein doesn't show such a switching, confirming that the FRET occurs only when the fluorophore is conjugated with the molecule. The switching ratio of the fluorescence was found to be  $\sim$ 85%. This is in agreement with a theoretical value of 84% calculated on the basis of the Förster formalism<sup>42</sup> with R= 24 Å and the orientational factor k = 0.67.



**Figure S3:** (a) Absorption spectrum of SLAC in the oxidized (red) and the reduced form (black). The emission spectrum of the fluorophore Atto 647N (blue) overlaps with absorption of the protein (hatched area) which is characteristic of the T1 Cu. (b) Fluorescence response of the K204C variant labeled with Atto647N when cycled between the reduced (high intensity, no FRET) and the oxidized (low intensity, high FRET) state using ascorbate for reduction under anaerobic condition and air for oxidation. This process can be repeated many times as shown above. Fluorophore only doesn't show any switching in these conditions.

Functionalization of coverslips: 0.17mm thickness (#1.5H) glass coverslips (Marienfield) were used for all immobilizations. The coverslips were first rinsed with acetone and water and then treated for 1 minute with 5% Hydrofluoric acid (HF) inside a fume hood.<sup>43</sup> (Caution: HF is an extremely dangerous chemical and proper training is required before handling it.) Immediately afterwards, they were rinsed several times with milliQ water and then treated with

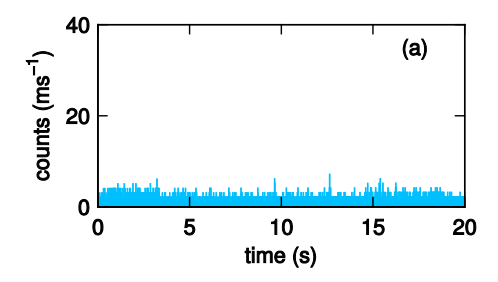
H<sub>2</sub>O/NH<sub>4</sub>OH/H<sub>2</sub>O<sub>2</sub> (5:1:1) bath at 70 °C. The coverslips were then rinsed several times with water and finally with ethanol. They were then flamed and used immediately for the next step or stored inside a desiccator until further use. The coverslips thus prepared contain active silanol groups which can readily react with silanes providing capability to functionalize the surface. The coverslips 1% for 30 minutes with solution 3 - (2 were aminoethyl)aminopropyl trimethoxysilane in methanol containing 5% glacial acetic acid and afterwards washed extensively with methanol. Thereafter, they were dried with a gentle flow of clean nitrogen and then left in the desiccator overnight. The following day coverslips were treated with a 5 mg/ml solution of methoxy-peg-NHS (MW 2000, Laysan Bio) and biotin-peg-NHS (MW 3400, Laysan Bio) (NHS: N-hydroxysuccinimide) in 50mM sodium phosphate buffer at pH 8. The ratio of methoxy to biotin peg was kept at or below 1000:1 to ensure only few biotin functionalities are present on the surface. The treatment continued for 8-10 hours or overnight and then the coverslips were washed extensively with water and dried with a gentle flow of clean nitrogen. The coverslips thus functionalized were used immediately for protein immobilization or kept desiccated at -20 °C until required.

Protein Immobilization: The functionalized coverslips were placed in a sample holder and incubated with 20mM MOPS buffer (pH 7.4) for 5–10 minutes. The buffer was then removed and a drop of NeutrAvidin (0.1mg/ml, Pierce) was applied to the coverslip. After 1 minute the coverslip was washed with excess buffer to remove unbound NeutrAvidin. The dye–protein conjugate (10–30 pM) was then applied to the surface to obtain the desired density of molecules and allowed to stand for 1 min. The unbound protein was then removed by washing with excess buffer taking care not to withdraw the entire buffer from the top of the coverslip as it was found that enzyme denatured at the air interface. The sample thus prepared was imaged on a confocal microscope to locate single molecules of the protein.

**Confocal Microscope:** Single molecule fluorescence measurements were performed on a home built confocal microscope. A pulsed laser emitting at 639 nm was controlled by PDL 800–B (PicoQuant) laser driver at 40MHz repetition

rate. The beam was passed through a narrow band clean-up filter (LD01-640/8-25, Semrock) and coupled into a single mode optical fiber (OZ Optics). The beam was collimated to the desired diameter with an aspheric lens of suitable focal length near the fiber end and reflected via a dichroic mirror (ZT640RDC, Chroma) to an infinity corrected high numerical aperture (NA) oil immersion objective (1.4 NA, 100X oil, Zeiss). The sample to be imaged was mounted on a scanning stage controlled by nanopositioning piezo elements (P517.3CD, Physik Instrumente). The emission was collected through the same objective and filtered through an emission filter (ET655LP, Chroma) to clean up the reflected and scattered light that passes through the dichroic. The emission was then focused onto a 75 µm pinhole to filter the background and then on the active area of a single photon counting module (SPCM-AQR-14, Perkin Elmer). Data acquisition was performed by a photon counting PC-board (TimeHarp 200, PicoQuant) in the time-tagged-time-resolved mode. The hardware and data acquisition were controlled by using the software SymPhoTime (PicoQuant).

Data collection: The sample to be scanned was mounted on a scanning stage and was brought into the focal plane of the objective. The images of typically (40 x 40) (µm)2 were recorded as x-y scans to locate single isolated SLAC molecules. To collect data from a single molecule, the laser was parked at one of the spots and measurement was made for 30 seconds to 5 minutes. One drawback of this method is that due to their limted photostability many fluorophores bleach within a few seconds. Thus, only the time traces containing more than 20 transitions between the upper and lower states were included for further analysis. A number of tests were performed to make sure that the observed fluctuations in the fluorescence intensity were not due to photophysics of the dye or to ET between the Cu and the dye. Firstly, in the absence of substrate, a stable signal corresponding to the low fluorescence state is observed and we did not encounter any dye photophysics (Figure S4a) under aerobic conditions (removal of the oxygen resulted in pronounced blinking of the dye in the presence as well as in the absence of reductant). This also ruled out that ET from the excited dye to the T1 Cu(II) center was responsible for the observed fluorescence intensity fluctuations. Secondly, under aerobic conditions a stable high fluorescence signal was observed in the presence of substrate and potassium



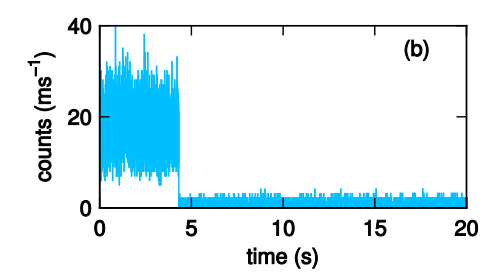


**Figure S4:** Binned time traces observed under aerobic conditions of (a) SLAC molecule in the oxidized state in the absence of DMPD and ascorbate. (b) SLAC molecule in the reduced state in the presence of DMPD (5mM), ascorbate (10mM) and KCN (1mM).

cyanide (KCN). KCN selectively and irreversibly inhibits the reaction of the enzyme with  $\mathrm{O}_2$  at the TNC so that the enzyme can not turn over  $^{44}$  and the T1 Cu stays reduced leading to a high fluorescence signal (Figure S4b). This result ruled out that ET from the reduced T1 Cu(I) center to the excited dye was responsible for the observed fluorescence intensity fluctuations. It is conceivable that KCN affects the activity of the T1 site and that in the absence of KCN still ET from the Cu(I) to the dye label may occur. We verified from the bulk kinetics assays that the enzyme is completely inhibited by 1mM KCN. In a related experiment we observed that addition of 1 mM KCN to an aerobic solution of ~80 µM of SLAC diminished the 330 nm absorption band typical of the oxidized T3 Cu pair in the TNC while the 600 nm absorption due to the oxidized T1 site was not affected (Figure S5). Addition of 500µM ascorbate and ~5µM DMPD quickly and completely abolished the 300 nm and 600 nm absorptions, indicating complete reduction of the protein, which is otherwise not possible in the presence of O<sub>2</sub> (Figure S5). Finally, the T1 Cu absorption at 600 nm was recovered by addition of ~1mM K<sub>3</sub>[Fe(CN)<sub>6</sub>] (Figure S5). We conclude that KCN selectively inhibits the O2 binding at TNC while the T1 site can still reversibly be reduced and oxidized, which is consistent with previous studies.<sup>44</sup> To make sure that the dye doesn't show any critical behavior in the presence of substrate, NeutrAvidin, which cannot turnover, was labeled with the same dye and the fluorescence was also checked in the presence of substrate. Alternatively, Atto647N-biotin which consists of a biotin moiety linked to the fluorophore was used on the NeutrAvidin functionalized coverslips. In both cases no fluctuations

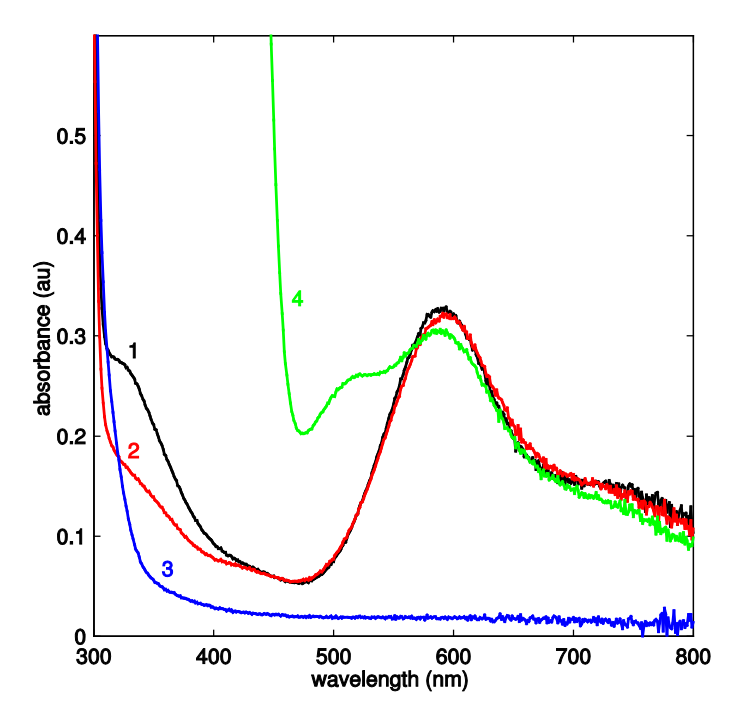


**Figure S5**: (1) Absorption spectra of resting SLAC in air saturated 200mM sodium phosphate buffer (pH 7.4) at ambient temperature; (2) 1 mM KCN added to 1; (3) 500  $\mu$ M ascorbate and 5  $\mu$ M DMPD added to 2; and (4) 1 mM K<sub>3</sub>[Fe(CN)<sub>6</sub>] added to 3.

in fluorescence were observed under aerobic conditions and in the presence of reductant and the traces similar to those shown in Figure S4b were observed. Only when the substrate is present in the solution above the immobilized SLAC, time traces like the ones shown in Fig 2a (main manuscript) were observed.

Data analysis: Data analysis was performed using MATLAB and C in three steps. In the first step the traces containing count rates less than 300 Hz were discarded and the remaining ones were binned and inspected one by one. Binning was performed only to visualize the data. Then the markers were set up to mark the portion of the time trace which contained useful information and to separate it from the remainder where, for example, the fluorophore had bleached. This was necessary for the second step when the raw time traces were submitted to the changepoint algorithm kindly provided by Prof. Haw Yang (Princeton University, USA). The algorithm is bin–free and uses a recursive binary segmentation of a trajectory (containing only photon arrival times) and

uses several statistical tests to determine the maximum number of changepoints where the count rate changes with a certain confidence interval. We can choose in the beginning the confidence intervals on the type-I (false positive) and the type-II (false negative) errors. We chose the values that suited best the description of our data while still preserving information about the fast dynamics. Complete details about the algorithm have been published elsewhere.<sup>33</sup> The estimated error rate in the changepoint determination amounts to 1% or less.<sup>45</sup> The spurious dynamics that are not associated with the activity of enzyme are taken care of during the next step of the analysis. Basically, by applying this algorithm, we have filtered the poissonian noise from the data and assigned intensity levels, and this results in traces as shown in Fig 2b red trace (main manuscript). In the next step, dwell times of the molecule in the on or off state were obtained and binned in the form of a histogram. The data could be well fitted with a single exponential. The first time bin contains the most uncertainty and was not used when fitting the data. Analysis of dwell times in the on state provided the decay rate of the on state  $(k_{on})$  which is equal to the electron transfer rate constant  $(k_{T1\to TNC})$  from T1 Cu to TNC. Similar analysis of the dwell times in the off state provided the decay rate of the off state ( $k_{
m off}$ ) which equals the sum of the rate of electron transfer from TNC to T1 Cu  $(k_{TNC\rightarrow T1})$ and the rate of reduction by DMPD:  $k_{\text{off}} = k_{\text{TNC} \to \text{T1}} + k_{\text{S}}[\text{DMPD}]$  in which  $k_{\text{S}}$  is the second order rate constant for the reduction of the T1 Cu by DMPD (see also Figure S6).

The rate constants were combined in histograms whereby each individual k value was weighed by the inverse of its variance as obtained from the exponential fit of the dwell times. Thus, the time traces which contained a low number of transitions due to photobleaching received less weight because of low statistics. The logarithms of the rate constants appear to represent a bell shaped curve corresponding to a normal distribution of the free energy of activation (Figure S7).

The rates of forward electron transfer, thus, follow a lognormal distribution (see Figure 2d, main manuscript). Although histograms were plotted to visualize the distribution, the fitting was performed on the unbinned data. To demonstrate

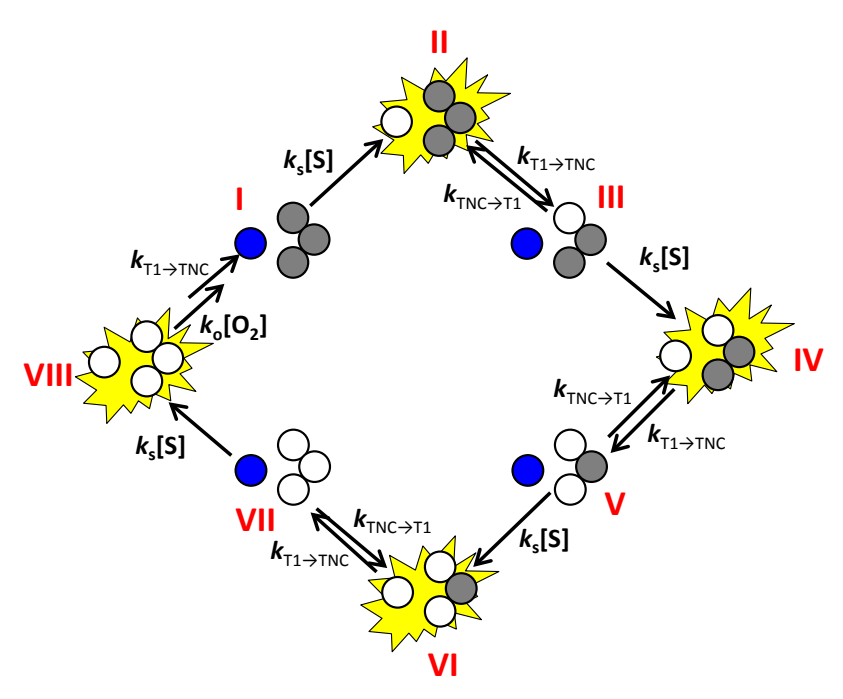


**Figure S6:** Cartoon representation of the enzyme cycle highlighting the sequential electron transfer steps. Oxidized T1 Cu is depicted in dark blue and the oxidized Cu's in the TNC in grey. Reduced Cu sites are depicted colorless. The fluorescence emission state of the molecule is shown as a bright yellow star, i.e. when the T1 Cu is reduced. Oxygen binding is supposed to occur, in this scheme, in state VIII but may also occur earlier, for instance in state V, VI or VII.

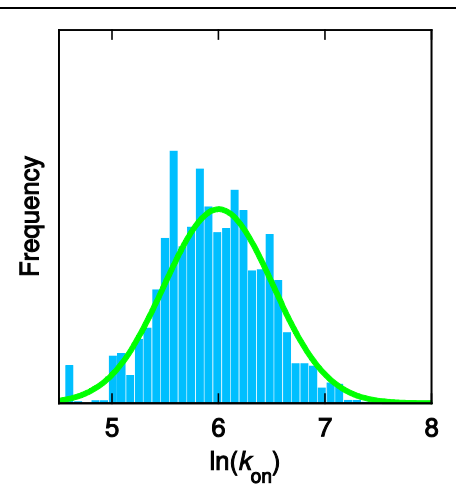


**Figure S7:** Distribution of log  $k_{\text{on}}$  values corresponding to the data shown in Figure 2d of main manuscript. The green line is the fit to the corresponding normal distribution.

that the distribution of  $k_{\rm on}$  is independent of the substrate concentration, the distribution of rates measured at 50 µM and 5mM DMPD concentration are shown in Figure S8(a, b). It is evident that the mean and the distribution are essentially identical at the two concentrations even though the catalytic reaction rates at these concentrations are very different. Similarly, the distribution of  $k_{\rm off}$  at these two concentrations are shown in Figure S8(c, d). It can be clearly noticed that the  $k_{\rm off}$  distribution is dependent on substrate concentration as expected. We utilized these data to estimate the rate of back electron transfer (from TNC to T1 Cu) and the second order rate constant for the reduction of T1 Cu by DMPD.

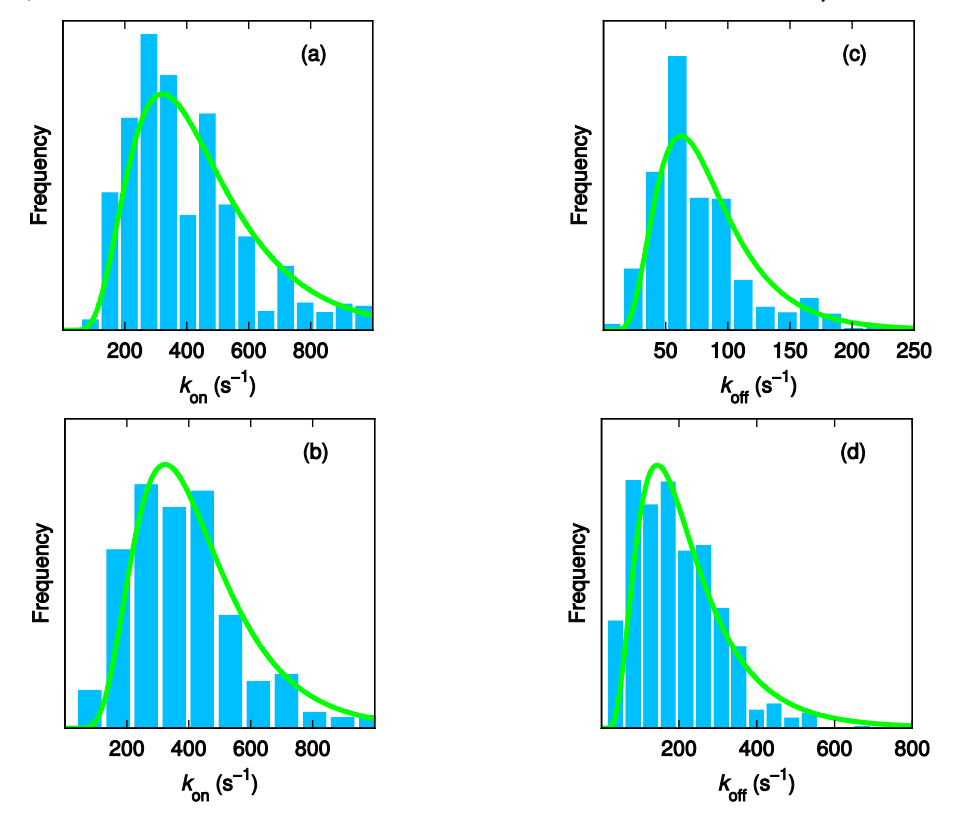


**Figure S8:** The distribution of ET rates across many molecules at different substrate concentrations. Distribution of (a)  $k_{\rm on}$  across 176 individual molecules at 50  $\mu$ M DMPD and (b) across 196 individual molecules at 5 mM DMPD concentration. (c) and (d) represent the distribution of  $k_{\rm off}$  for the same molecules as shown in (a) and (b). Notice the different horizontal scales in (c) and (d). Ascorbate concentration = 10mM. The green lines are fits to the data corresponding to a lognormal distribution although, strictly speaking, (c) and (d) are the sum of two lognormal distributions.

Calculation of the reorganization energy ( $\lambda_{TOT}$ ): The semiclassical expression of Marcus theory was used which is given by:<sup>46</sup>

$$k_{et} = \sqrt{\frac{4\pi^2}{h^2 \lambda RT}} H_{DA}^2 exp \left\{ -\frac{(\Delta G^0 + \lambda)^2}{4\lambda RT} \right\}$$

Where  $\lambda$  is the reorganization energy,  $H_{DA}$  is the electronic coupling matrix element between the donor and the acceptor and  $-\Delta G^0$  is the driving force. The activationless ET rate  $(k^0)$  was calculated by using the following expression in context of the Marcus theory.

$$k^0 = 10^{13} exp\{-\beta(r-r_0)\}$$

where  $\beta$  is the distance dependence of the decay of  $H_{AB}$  having a value of 1 Å<sup>-1</sup>,<sup>37</sup> r is the distance between the donor and the acceptor and  $r_{\theta}$  is the distance where the  $k^0$  reaches a value of  $10^{13}$  (2.8 Å).

Thus, the simplified form of the Marcus equation can be written as

$$k_{et} = k^0 exp \left\{ -\frac{\Delta G^{\ddagger}}{RT} \right\}$$

which provides the activation energy ( $\Delta G^*$ ) and the associated uncertainty, with

$$\Delta G^{\ddagger} = \frac{(\Delta G^0 + \lambda)^2}{4\lambda}$$

from where the reorganization energy and the associated uncertainty were estimated.

#### 4.4 References

- [1] Farver, O.; Pecht, I. Coord. Chem. Rev. 2011, 255, 757.
- [2] Farver, O.; Wherland, S.; Pecht, I. J. Biol. Chem. 1994, 269, 22933.
- [3] Tollin, G.; Meyer, T. E.; Cusanovich, M. A.; Curir, P.; Marchesini, A. *Biochim. Biophys. Acta* **1993**, *1183*, 309.
- [4] Special Issue on Single-Molecule Spectroscopy. Acc. Chem. Res. 2005, 38, 503.
- [5] English, B. P.; Min, W.; van Oijen, A. M.; Lee, K. T.; Luo, G.; Sun, H.; Cherayil, B. J.; Kou, S. C.; Xie, X. S. *Nat. Chem. Biol.* **2006**, *2*, 87.
- [6] Smiley, R. D.; Hammes, G. G. Chem. Rev. 2006, 106, 3080.
- [7] van Oijen, A. M.; Loparo, J. J. *Annu Rev Biophys* **2010**, *39*, 429.
- [8] Lu, H. P.; Xun, L.; Xie, X. S. Science 1998, 282, 1877.
- [9] Pudney, C. R.; Lane, R. S.; Fielding, A. J.; Magennis, S. W.; Hay, S.; Scrutton, N. S. *J. Am. Chem. Soc.* **2013**, *135*, 3855.
- [10] Kuznetsova, S.; Zauner, G.; Aartsma, T. J.; Engelkamp, H.; Hatzakis, N.; Rowan, A. E.; Nolte, R. J.; Christianen, P. C.; Canters, G. W. Proc. Natl. Acad. Sci. U. S. A. 2008, 105, 3250.
- [11] Goldsmith, R. H.; Tabares, L. C.; Kostrz, D.; Dennison, C.; Aartsma, T. J.; Canters, G. W.; Moerner, W. E. Proc. Natl. Acad. Sci. U. S. A. 2011, 108, 17269.
- [12] Tabares, L. C.; Kostrz, D.; Elmalk, A.; Andreoni, A.; Dennison, C.; Aartsma, T. J.; Canters, G. W. *Chem. Eur. J.* **2011**, *17*, 12015.
- [13] Zhang, Z.; Rajagopalan, P. T.; Selzer, T.; Benkovic, S. J.; Hammes, G. G. Proc. Natl. Acad. Sci. U. S. A. 2004, 101, 2764.
- [14] Solomon, E. I.; Sundaram, U. M.; Machonkin, T. E. *Chem. Rev.* **1996**, *96*, 2563.
- [15] Solomon, E. I.; Augustine, A. J.; Yoon, J. Dalton Trans. 2008, 3921.

- [16] Farver, O.; Wherland, S.; Koroleva, O.; Loginov, D. S.; Pecht, I. *FEBS J.* **2011**, *278*, 3463.
- [17] Farver, O.; Tepper, A. W.; Wherland, S.; Canters, G. W.; Pecht, I. *J. Am. Chem. Soc.* **2009**, *131*, 18226.
- [18] Wherland, S.; Farver, O.; Pecht, I. *ChemPhysChem* **2005**, *6*, 805.
- [19] Kuznetsova, S.; Zauner, G.; Schmauder, R.; Mayboroda, O. A.; Deelder, A. M.; Aartsma, T. J.; Canters, G. W. *Anal. Biochem.* **2006**, *350*, 52.
- [20] Machczynski, M. C.; Vijgenboom, E.; Samyn, B.; Canters, G. W. *Protein Sci.* **2004**, *13*, 2388.
- [21] Skalova, T.; Dohnalek, J.; Ostergaard, L. H.; Ostergaard, P. R.; Kolenko, P.; Duskova, J.; Stepankova, A.; Hasek, J. *J. Mol. Biol.* **2009**, 385, 1165.
- [22] Skalova, T.; Duskova, J.; Hasek, J.; Stepankova, A.; Koval, T.; Ostergaard, L. H.; Dohnalek, J. Acta Crystallogr., Sect. F: Struct. Biol. Cryst. Commun. 2011, 67, 27.
- [23] Nakamura, K.; Go, N. Cell. Mol. Life Sci. 2005, 62, 2050.
- [24] Tepper, A. W. J. W.; Milikisyants, S.; Sottini, S.; Vijgenboom, E.; Groenen, E. J. J.; Canters, G. W. *J. Am. Chem. Soc.* **2009**, *131*, 11680.
- [25] Gupta, A.; Nederlof, I.; Sottini, S.; Tepper, A. W.; Groenen, E. J.; Thomassen, E. A.; Canters, G. W. *J. Am. Chem. Soc.* **2012**, *134*, 18213.
- [26] See Supporting Information
- [27] Wong, L. S.; Khan, F.; Micklefield, J. Chem. Rev. 2009, 109, 4025.
- [28] Heering, H.; Canters, G. Engineering the Bioelectronic Interface: Applications to Analyte Biosensing and Protein Detection; Davis, JJ, Ed 2010, 120.
- [29] Durán, N.; Rosa, M. A.; D'Annibale, A.; Gianfreda, L. Enzyme Microb. Technol. 2002, 31, 907.

- [30] Prime, K. L.; Whitesides, G. M. Science 1991, 252, 1164.
- [31] Ha, T.; Rasnik, I.; Cheng, W.; Babcock, H. P.; Gauss, G. H.; Lohman, T. M.; Chu, S. *Nature* **2002**, *419*, 638.
- [32] Rasnik, I.; Myong, S.; Cheng, W.; Lohman, T. M.; Ha, T. *J. Mol. Biol.* **2004**, *336*, 395.
- [33] Watkins, L. P.; Yang, H. J. Phys. Chem. B 2005, 109, 617.
- [34] McKinney, S. A.; Joo, C.; Ha, T. Biophys. J. 2006, 91, 1941.
- [35] Tepper, A. W. J. W.; Aartsma, T. J.; Canters, G. W. Faraday Discuss. **2011**, *148*, 161.
- [36] Strange, R. W.; Murphy, L. M.; Dodd, F. E.; Abraham, Z. H.; Eady, R. R.; Smith, B. E.; Hasnain, S. S. *J. Mol. Biol.* **1999**, *287*, 1001.
- [37] Gray, H. B.; Winkler, J. R. Q. Rev. Biophys. 2003, 36, 341.
- [38] Voityuk, A. A. J. Phys. Chem. B 2011, 115, 12202.
- [39] Heppner, D. E.; Kjaergaard, C. H.; Solomon, E. I. *J. Am. Chem. Soc.* **2013**, *135*, 12212.
- [40] Salverda, J. M.; Patil, A. V.; Mizzon, G.; Kuznetsova, S.; Zauner, G.; Akkilic, N.; Canters, G. W.; Davis, J. J.; Heering, H. A.; Aartsma, T. J. *Angew Chem Int Ed Engl* **2010**, *49*, 5776.
- [41] Davis, J. J.; Burgess, H.; Zauner, G.; Kuznetsova, S.; Salverda, J.; Aartsma, T.; Canters, G. W. *J. Phys. Chem. B* **2006**, *110*, 20649.
- [42] Lakowicz, J. R. *Principles of Fluorescence Spectroscopy*; Springer, 2007.
- [43] Betzig, E.; Patterson, G. H.; Sougrat, R.; Lindwasser, O. W.; Olenych, S.; Bonifacino, J. S.; Davidson, M. W.; Lippincott-Schwartz, J.; Hess, H. F. *Science* **2006**, *313*, 1642.
- [44] Meyer, T. E.; Marchesini, A.; Cusanovich, M. A.; Tollin, G. *Biochemistry* **1991**, *30*, 4619.

- [45] Terentyeva, T. G.; Engelkamp, H.; Rowan, A. E.; Komatsuzaki, T.; Hofkens, J.; Li, C. B.; Blank, K. ACS Nano 2012, 6, 346.
- [46] Marcus, R. A.; Sutin, N. Biochim. Biophys. Acta 1985, 811, 265.